System Identification Modeling for Flight Control Design

Christina M. Ivler
Aerospace Engineer

Mark B. Tischler
Flight Control Group Lead

Aeroflightdynamics Directorate (AMRDEC)

US Army Research, Development, and Engineering Command
Ames Research Center, Moffett Field, CA

Abstract

Flight control analyses require accurate models of the bare airframe and its associated uncertainties, as well as the integrated system (block diagrams) across the frequency range of interest. Frequency domain system identification methods have proven to efficiently fulfill these requirements in recent rotorcraft flight control applications. This paper presents integrated system identification methods for flight control modeling for flight test examples of the Fire Scout MQ-8B, S-76, and ARH-70A. The paper also looks toward how system identification could be used in new modeling challenges such as the Joint Heavy Lift rotorcraft as well as small unique unmanned configurations.

Nomenclature

a_x, a_y, a_z	accelerometer components in body-axis
a_{x_m}, a_{y_m}	accelerations as measured at the sensor, not at the center of gravity
p,q,r	angular rates
T	engine torque
u,v,w	body-axis velocities
u_m, v_m	velocities as measured at the sensor, not at the center of gravity
u	vector of controls in state-space model
M, F, G, H_0, H_1	state-space model terms
x	vector of states in state-space model
x_e	engine delay state, used for padé approximation
β_o	

Presented at the RAeS Rotorcraft Handling-Qualities Conference, University of Liverpool, UK, 4-6 Nov 2008

$\mu_{wb-ail}\,\delta_{ail}$	derivative relating asymmetric wing bending to aileron input
ϕ, θ, ψ	Euler angles
Φ_{p1}	bending mode displacement coefficient
σ	standard deviation
τ_f	flapping time constant
υ	inflow
υ_ζ	regressive lag frequency in the rotating frame
ω_c	cross-over frequency
Ω_R	rotor speed with respect to the fuselage

Introduction

Most flight control design methodologies require a linear model that accurately represents the aircraft that is to be controlled. For example, classical feedback design (root locus), quantitative feedback theory, LQR, eigenstructure-assignment, and linear dynamic inversion techniques are all examples of control techniques that use linear state-space models or transfer functions. Additionally, linear models are also used in direct parametric optimization techniques such as CONDUIT® (Ref. 1). When a prototype aircraft is available, frequency domain system identification can be used to develop state-space models directly from flight data (Ref. 2). This method has been proven to be highly accurate and efficient, and also has the benefit of providing uncertainty parameters.

Frequency domain system identification has been used to develop linear vehicle models for many recent rotorcraft applications such as the CH-47 (Ref. 3), ARH (Ref. 4), S-76 (Ref. 5), UH-60MU (Ref. 6), and Fire Scout (Ref. 7). In most cases, these system identification models were used for flight control designr dynamicat27 6(g)-3, qsthicle m3 Tw[(idcsicle)6(phy)12cases, tuo9n TD0. 7

sweep. Finally, the frequency range of accuracy is improved by combining a weighted average of multiple windows, in a method known as Composite Windowing. The result is a high quality MIMO frequency response database.

2. State space model identification

A state-space model structure is chosen by the user, based on analysis of the frequency responses. Then, the freed state-space model para

control analysis.

Aircraft subsystems must be validated – The use of frequency sweeps in flight can be used to identify broken and closed loop responses of the aircraft with the control system. If the open loop and closed loop flight frequency responses match those from the block diagram (which includes the aircraft linear model and subsystem models), then the block diagram subsystems can be assumed to be validated. If the broken and closed loop responses do not match, identification of individual subsystems on the aircraft can be carried out until the source of the mismatch is determined.

Case Studies for Integrated System Identification and Flight Control

A series of case studies are shown to exemplify how system identification was used to meet the flight control requirements given in the previous section for recent rotorcraft flight control development applications. Three different case studies are given; MQ-8B Fire Scout UAV, S-76D, and the ARH-70A. For these case studies, creative modeling solutions were found in order to meet the flight control requirements. This trio of case studies demonstrates the flexibility of the method and the variety of the ways in which it has been successfully used.

Fire Scout

The Fire Scout is being developed as a ship-based VTOL UAV for the U.S. NAVY. The MQ-8B, which is the current version of the Fire Scout, has an upgraded transmission, four rotor blades (as opposed to three on the earlier configuration, RQ-8A), and minor modifications to the airframe as compared to the RQ-8A. The MQ-8B Fire Scout is depicted in Fig. 1.

Figure 1. MQ-8B first hover (reprinted from Ref. 7).

responses were well predicted with the presented model

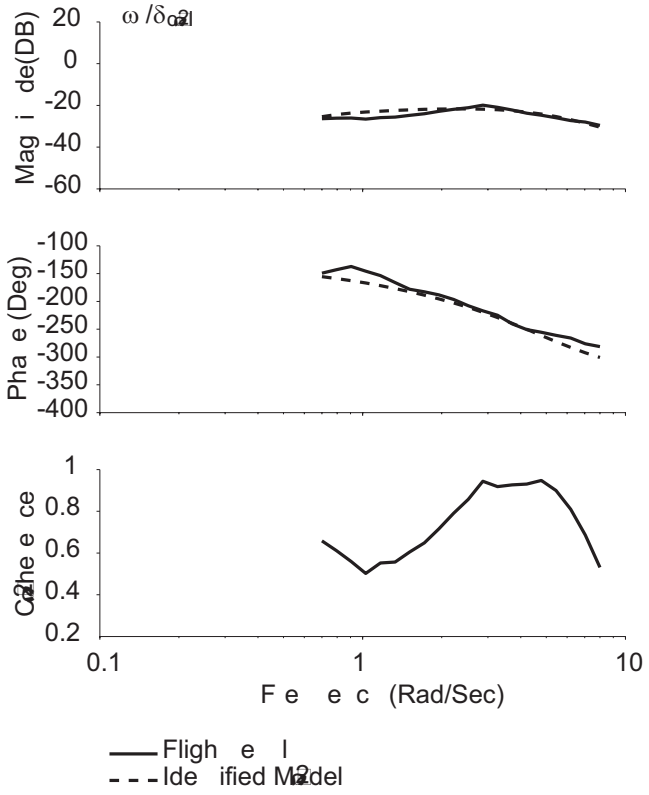
ω /δ
Mag i de(DB)
20
0
-20
-40
-60
Pha e (Deg)
-100
-150
-200
-250
-300
-350
-400
Coh e ce
1
0.8
0.6
0.4
0.2
0.1
1
10
F e e c (Rad/Sec)
Fligh e l
Ide ified Model

Inner Loop Control Law Design

After the model was identified and verified to be accurate, the next step in the process was to perform control design. The inner loop architecture was a basic attitude command attitude hold PID-type control system for pitch, roll, and yaw. The vertical axis was a rate command system implemented as a PI controller on the vertical velocity, with a torque feedback loop. Two methods of control law optimization were used – the CONDUIT® software developed by AFDD and an NGC implemented genetic algorithm. Both methods utilized the identified linear models. The results of the optimizations were compared to provide confidence in the control law design results. Table 1 shows the specifications that were considered key in the optimizations. The results of the two optimizations turned out very similar, as shown in Table 2, and thus provided confidence in the flight control design.

Once the control law design was optimized and cross-checked between the two design methodologies, the next step was to test the performance of the system under uncertain conditions.

Table 1. Key MQ-8B Specifications.

Specification	Description
Stability Margins	Ensures that stability margins are met for the nominal control system design.
ADS-33 Bandwidth	Ensures that the UAV meets piloted bandwidth requirements since it is a full sized rotorcraft, and good flying qualities are desired even though it is not piloted.
Disturbance Rejection Bandwidth	Ensures that the system will reject disturbances. This is very important for ship operations of a UAV.
Damping Ratio	Ensures that lightly damped oscillations are not allowed. This is important for precision operations.
Cross-over Frequency	Ensures that the cross-over frequency of the system is minimized (CONDUT®) to ensure actuators are not overused. For Genetic algorithms, user checks that cross-over frequency is reasonable.

Table 2. Comparison of CONDUIT® and genetic algorithm designs for MQ-8B.

	Pitch G.M. (dB)	**Pitch P.M. (deg)**	**Roll G.M. (dB)**	**Roll P.M. (deg)**	**Yaw G.M. (dB)**	**Yaw P.M. (deg)**	**Collective G.M. (dB)**	**Collective P.M. (deg)**
CONDUIT®	8.5	46.1	8.32	48.7	16.7	45	7.1	45
Genetic	9.3	40.5	6.4	42	8.1	49.8	22.7	44.9
	Pitch Crossover (rad/s)	**Roll Crossover (rad/s)**	**Yaw Crossover (rad/s)**	**Collective Crossover (rad/s)**	**Pitch D.R.B. (rad/s)**	**Roll D.R.B. (rad/s)**	**Yaw D.R.B. (rad/s)**	**Collective D.R.B. (rad/s)**
CONDUIT®	3.92	4.18	2.82	2.14	0.96	1.4	1.1942	0.98
Genetic	3.39	4.68	4.98	2.2	.949	1.75	1.21	1.209

G.M. = gain margin, P.M. = phase margin, D.R.B. = disturbance rejection bandwidth

Uncertainty Analysis

For Fire Scout, uncertainties in the identified stability and control derivatives were considered. For this parametric uncertainty analysis, the Cramer-Rao bounds of the individually identified parameters from the Fire Scout state-space model were considered. Cramer-Rao bounds represent the theoretical accuracy of the identified derivatives in the state-space model (Ref. 2). The Cramer-Rao bounds provided by CIFER® are scaled to represent the expected standard deviation in the identified parameters:

$$\left(CR_i\right)_{cifer} \approx \sigma_i \quad (14)$$

Thus, there was a direct measure of the uncertainty for each identified parameter in the state-space model. The effect of these uncertainties on the stability of the system was analyzed for the hover control laws. In order to take into account a 99.7% confidence interval, each derivative that has an associated Cramer-Rao bound was randomly perturbed by $+/-3\sigma$. The random term only determines whether the derivative should be perturbed positively or negatively, not the absolute size of the perturbation, which was fixed at $|3\sigma|$. Using this method, there are a finite number of possible perturbed models - $2^{(\#\,free\_\,parameters)}$. However, with 32 free parameters in the hover model, there were 4.29E9 possible perturbed models. By randomly perturbing all derivatives at one time and then looking at the effect on the stability, one can determine how severely the combinations of uncertainty affect the system and whether more robustness needs to be built into the control laws.

CONDUIT®

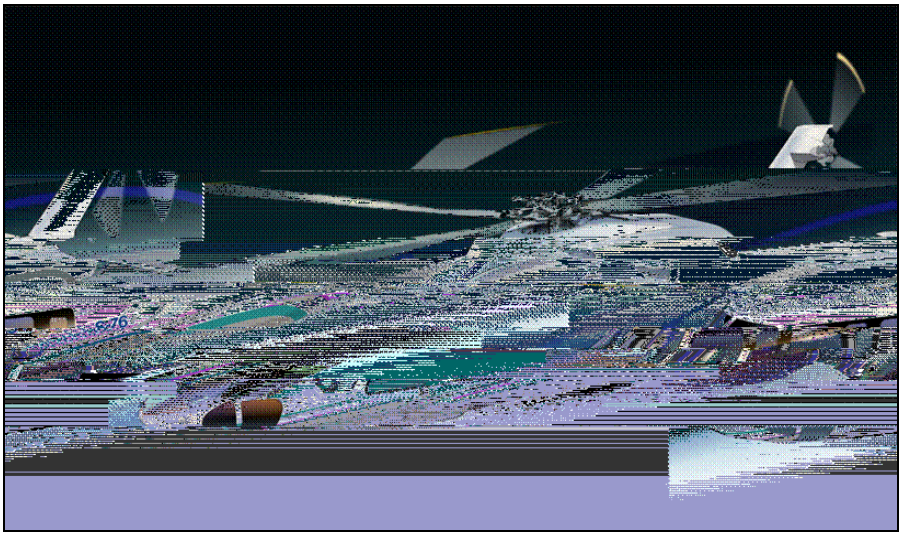

Figure 7. S-76D.

S-76

The S-76 is a light twin-engine, four bladed helicopter that has been operating since the 1970s. The newest upgrade, the S-76D, will feature a Thales automatic flight control system (AFCS). The S-76D is pictured in Fig. 7.

In order to develop an automatic flight control system, the S-76 team was required to provide accurate models of the aircraft to the Thales AFCS developers. Because the S-76D was not ready for flight the S-76C, which is a similar design, was used for the initial system identification of the helicopter. This model would be used for initial AFCS design, and later updated versions of the models would be created after first flight. Thus, the key concerns for the S-76C team involved providing the best model possible for AFCS design. The following

$$u = \left[\delta_{lon} \quad \delta_{lat} \quad \delta_{ped} \quad \delta_{col}\right]^T \tag{18}$$

$$y = [\dot{u}_m \quad \dot{v}_m \quad \dot{w} \quad p \quad q \quad r \quad a_{x_m} \quad a_{y_m} \quad a_z \quad (a_{y_m})_2]^T \tag{19}$$

In the following section, examples comparing the higher order and quasi-steady models are shown to explain why the more complex model structures were needed. For the quasi-steady model only the fuselage states were included:

$$x = \left[u \quad v \quad w \quad p \quad q \quad r \quad \phi \quad \theta\right]^T \tag{20}$$

The use of the higher order model was a key factor in obtaining a valid model over a wide frequency range.

Flap/Fuselage Dynamics

The S-76 helicopter exhibits moderate blade flap stiffness, which indicates that the on-axis responses (q/δ_{lon} and p/δ_{lat}) were well modeled by a 6 DOF

Flight Data
Identified Hybrid Model (including lead-lag and flapping dynamic)
Identified 6 DOF Model

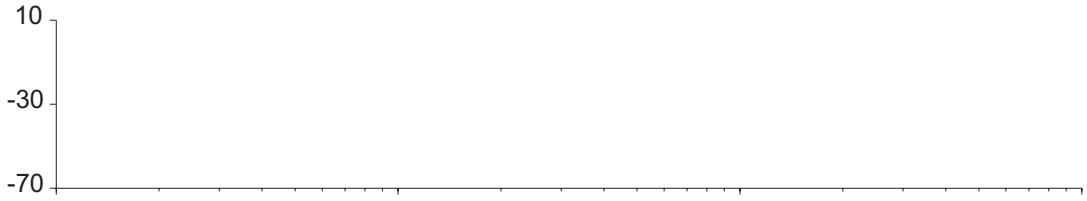

——Fligh Da a
- - -H b id M del (i cl di g e gi e d a ic ade a .)
- - - Q a i- ead 6DOF del

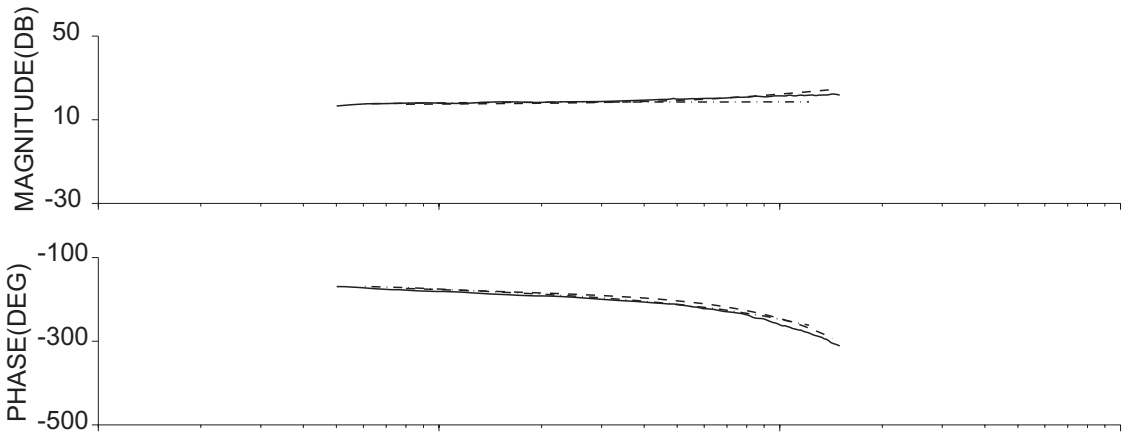
MAGNITUDE(DB)
50
10
-30
PHASE(DEG)
-100
-300
-500

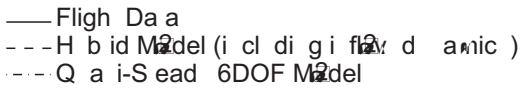
Fligh Da a
H b id M del (i cl di g i fla d a nic)
Q a i-S ead 6DOF M del

-304952566693246226177938253917813296177938253720939042 4873506QBT
-35
-40
5
0
-5

Ensuring physical fidelity of the model

Once the time domain verification was performed, it was important to analyze the S-76 model to ensure that it was physically meaningful. These checks were performed in order to meet the requirement that the model could be used to gain physical insight. The structure used on the S-76, a hybrid model, contains physically meaningful parameters since it was derived from the physics that govern the dynamics of a helicopter. For the S-76, some of these identified physical parameters were compared to theory - the flapping constant τ_f, the linear acceleration terms due to flapping $X_{\beta_{1c}}$ and $Y_{\beta_{1s}}$, and the rotating lag frequency, υ_ζ.

The flapping constant was an identified parameter. Its value was compared to the theoretical calculation (Ref. 2):

$$\frac{^{*}}{16} \quad 1 \quad \frac{8}{3} \qquad ^{1}$$

Figure 13. ARH-70A.

ARH

The Armed Reconnaissance Helicopter, ARH-70A, is being developed by Bell Helicopter to replace the OH-58. The ARH-70A is depicted in Fig. 13.

In order to meet the desire to achieve Level 1 handling qualities; the AFCS was designed to meet ADS-33E-PRF requirements. Flight identified models were developed and used in the AFCS design. The flight control requirements that were addressed through system identification included:

1. Determination and validation of accurate models for flight control design.

2. Validation of the control law block diagrams.

System identification played a key role in preparing for the flight control design of the ARH-70A. Models were identified from flight data at the following flight conditions: hover, level flight at maximum rate of climb airspeed, and level flight at 90% maximum speed with continuous power. The hover model identification and control block diagram validation will be given as examples of how system identification was used to meet ARH-70A flight control design requirements.

Model Identification at Hover

The ARH frequency sweep flight testing data was used to identify frequency-responses of the aircraft. The next step was to determine if a 6 DOF model structure was sufficient. Similarly to the Fire Scout, it was determined that since the rotor stiffness was moderate, and only moderate control cross-over frequencies were to be used, that the quasi-steady 6 DOF model was sufficient. Therefore the model structure takes the following form:

$$Mx \quad Fx + Gu$$

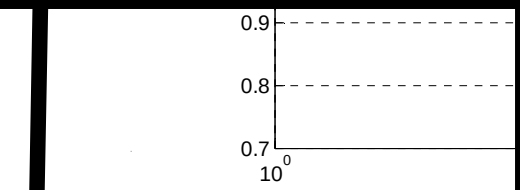
0.9
0.8
0.7
10^0

Validation of the control law block diagrams

Once the model was identified, the next step was to check that the block diagrams were correct by doing frequency response identification of the aircraft with control laws turned on. In an ideal situation, the block diagrams would be validated by doing a broken loop analysis from flight data and comparing to the block diagram. However, the required data to calculate a broken loop response were not available, so a validation of only the control law portion of the block diagram was performed. This ensures that the control laws are implemented correctly on the aircraft, which is an important part of ensuring that the control laws perform as expected. Considering that the model portion of the block diagram was already validated in the system identification, and that the linkages and actuators were well known, checking only the control law portion of the block diagram was a reasonable compromise.

MAGNITUDE(DB)
-10
-50
-90

Flight Data
CONDUIT

Future Challenges

System identification methods were very useful in resolving flight control challenges for the rotorcraft case studies presented in the previous sections. These rotorcraft however, are examples of upgrades or civilian aircraft that are being converted to military use. Thus, these aircraft are well known configurations that have been flying in some capacity for many years, and as such few real surprises in the dynamics arose during the system identification. Additionally, these aircraft are of average size and gross weight, for which the modeling, flight control, and handling qualities requirements and challenges are well known. Future configurations include the extremes of very large and very small aircraft, whose dynamics and handling qualities are not well known. The Joint Heavy Lift (JHL) program represents the extreme of a very large rotorcraft. On the other extreme, many small UAVs are being developed for use in

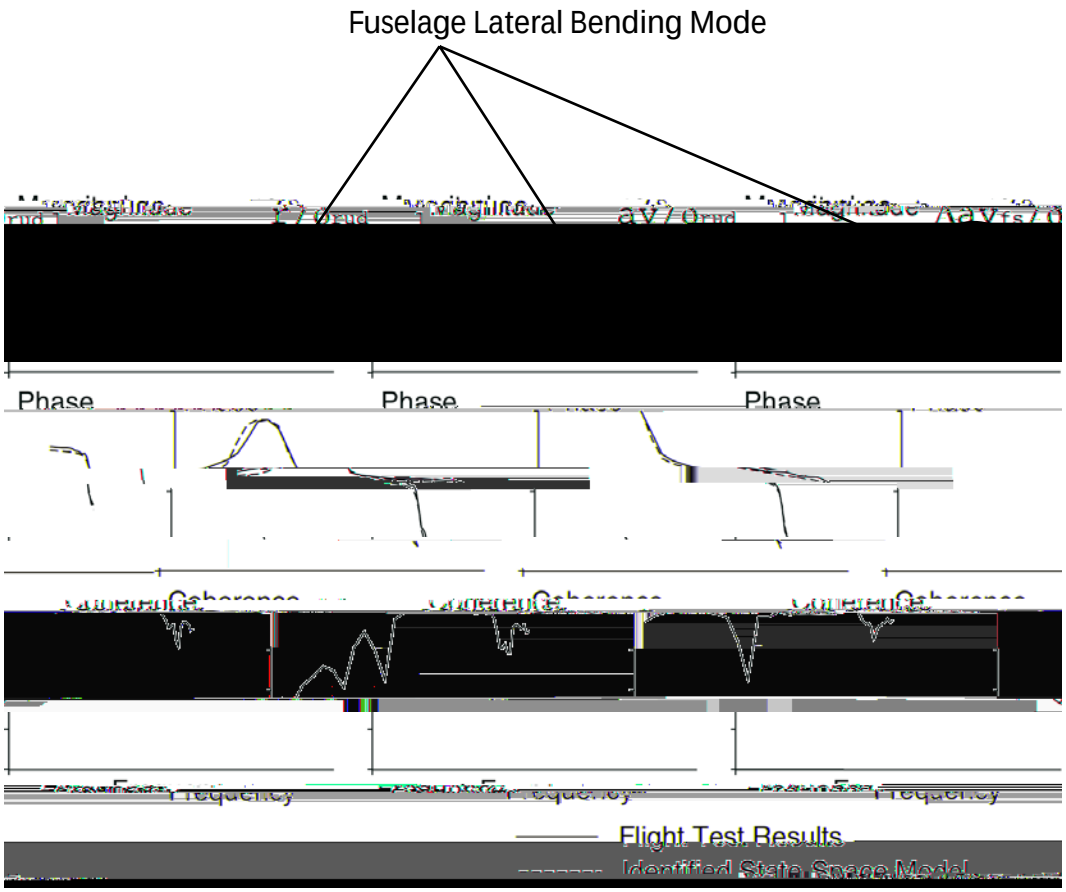

Figure 18. Comparison of model and flight data for lateral dynamics for a large transport aircraft (reprinted from Ref. 12).

Non-parametric Modeling of Structural Modes

Parametric modeling of all the structural and rotor-modes can be very time consuming due to the coupled and overlapping nature of these modes. A non-parametric analysis method can be used to replace the state-space model with a frequency response from flight data, which will contain the un-modeled modes (as long as it has good coherence at those modes), to generate a broken-loop response. Then stability margins can be accurately evaluated over the frequency range of the un-modeled modes. This could be used on the JHL to easily determine stability margins with respect to structural modes that are not included or accurately represented in the state-space model.

In the analysis, the block diagram should be setup similarly to that shown in Fig. 19. The broken loop is calculated by multiplying the flight identified frequency response with the control system frequency response. The state-space model is still in place for all off-axis inputs, and a single frequency response replaces the dynamics for the on-axis input/output response. This method ignores the effect of off-axis couplings on the calculated on-axis broken loop response, but these have a small effect when the off-axis loops are closed. This will produce an accurate broken loop response, which

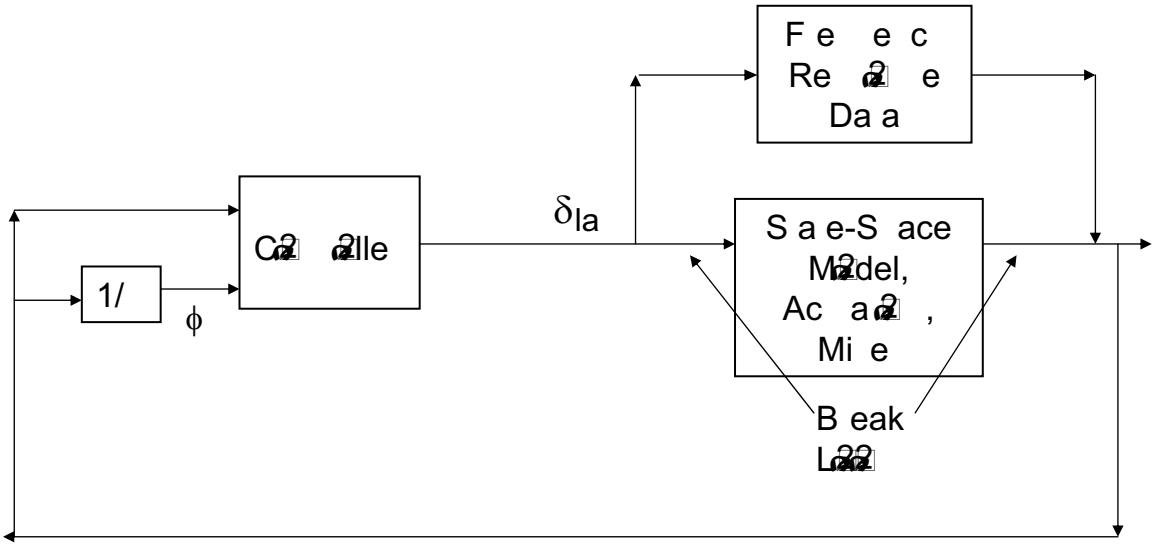

Figure 19. Block Diagram showing use of non-parametric model in flight control analysis.

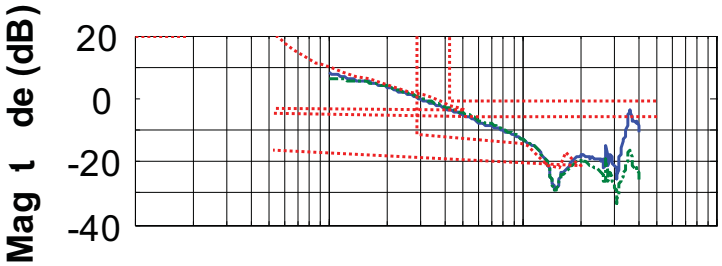

An uncertainty analysis of the non-parametric model

parametric models. Rapid system identification has been very useful for UAV applications in the past (Ref. 14). As example of this was rapid system identification of an R-50 helicopter in Ref. 14, which used coupled rotor-fuselage dynamics (similar to S-76) to achieve a good match in the roll rate response. A comparison between the R-50 flight data and the model is given in the paper, and is shown in Fig. 22. The results indicate that these higher-order modeling methods for large rotorcraft also work well on small rotorcraft, and provide a wide frequency range of accuracy.

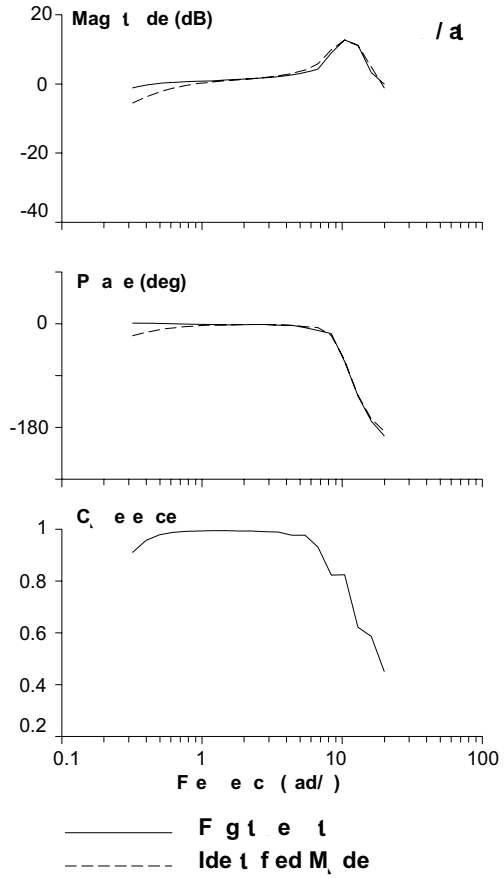

Figure 22. R-50 model and flight data comparison (reprinted from Ref. 14).